VIII International Conference on Fracture Mechanics of Concrete and Concrete Structures
FraMCoS-8
J.G.M. Van Mier, G. Ruiz, C. Andrade, R.C. Yu and X.X. Zhang (Eds)

SALT CRYSTALLIZATION-INDUCED DAMAGE OF CEMENT MORTAR MICROSTRUCTURE INVESTIGATED BY MULTI-CYCLE MERCURY INTRUSION

M. KONIORCZYK, P. KONCA AND D. GAWIN

Department of Building Physics and Building Materials
Technical University of Lodz, Łódź, Poland
e-mail: marcin.koniorczyk@p.lodz.pl, web page: http://kfb-lx.p.lodz.pl/

Key words: Cement mortar, Salt crystallization, Multi-cycle MIP, Durability, Pore structure

Abstract: The paper considers the change of cement mortar microstructures due to sodium sulfate crystallization. The pressure generated during the crystallization, causes the deterioration of the solid skeleton of cement-based materials. The magnitude of stress induced by crystals growing in the pores strongly depends on the geometry of the system. The influence of salt crystallization on the damage of internal structure was investigated for three types of cement mortar: without air-entraining admixture (AEA) and with 0.1% and 0.2% AEA. Most severe damage of cement mortar microstructure, was observed for samples without AEA. Pores of diameter 0.2-60 μm increased their volume up to 250%. The salt crystallization revealed the damage of pores, which diameter equals 0.6-30 μm, in samples containing 0.1% and 0.2% of AEA and the increase of pore volume never exceeded 155%. The additional pore volume, which appears in CM0 samples affected by salt crystallization, is created by micro-cracks generated during crystal growth. The salt crystallization significantly influence the volume and availability for water of capillary pores and therefore affect the transport properties and the durability of cement-based materials.

1 INTRODUCTION

Cement based materials are widely used in the contemporary civil engineering and they are exploited in more and more severe conditions. They are porous materials, which means, that they are built of the solid skeleton and the pores, which might be filled with the gaseous and the liquid phase. The liquid phase contains, besides the water, various types of contaminations, including salts. The contaminations migrate into the material through the system of interconnected pores. Therefore the knowledge about the porosity and the pore size distribution is extremely important considering the durability of the material [1].

The microstructure of analyzed cement mortar is investigated by means of the mercury intrusion test [2-4]. The technique is very simple in principles. It is assumed that the material contains the set of cylindrical pores of different dimension. Since the mercury is the non-wetting fluid, the pressure must be applied in order to intrude it into the pore system; the smaller are pores the higher pressure must be applied. For such the pore model, to assess the diameter of pores, which are currently intruded by the mercury, the Washburn equation may be applied [5]:

$$d = -\frac{4\gamma \cos\theta}{P} \tag{1}$$

where d is cylindrical pore diameter, which is being intruded, θ is advancing contact angle of mercury, γ is the surface tension of mercury and P is the applied pressure. One has

to remember that the MIP test gives information about the model of an internal structure, which is composed of the connected cylindrical pores, not about the real microstructure of cement-based material. Therefore the MIP method has some drawbacks, i.e. it underestimates the larger and overestimates the finer pores. These disadvantages are well recognized and described in the literature [6]. Most of them result from the fact that the majority of pores in the cementitious materials are connected with neighboring ones by thinner necks and they are called ink-bottle type pores. Some additional information about the pore shape, which partly overcomes the disadvantageous of the method, may be obtain by applying two mercury intrusion cycles [7, 8]. It was observed that after first mercury intrusion-extrusion cycle part of the mercury volume was entrapped in the pore system. The difference between the mercury volume intruded during the first ($V_{por}^{1\text{int}}$) and the second ($V_{por}^{2\text{int}}$) cycle might be the measure of the ink-bottle type pores contribution ($C_{ink-bottle}$) in the whole pore volume as a function of mercury pressure or a pore radius, according to the equation:

$$C_{ink-bottle}\left(r \geq r_0\right) = 1 - \frac{V_{por}^{2\text{int}}\left(r_0\right)}{V_{por}^{1\text{int}}\left(r_0\right)} \tag{2}$$

The above equation describes the contribution of ink-bottle type pores with diameter larger or equal to the considered pore diameter r_0.

Cement based materials are loaded not only with the external forces but also with the internal pressure, which might be created by the development of the expanding phases in the pore system, i.e. due to salt crystallization, ice formation, etc. In the presented paper the change of cement mortar microstructure due to the sodium sulfate crystallization was investigated using multi-cycle MIP. Three types of cement mortar were analyzed, the samples differ with the addition of the air-entraining admixture (AEA). Applying two mercury intrusion-extrusion cycles the change of the total porosity, the pore size distribution and the information about the pore shape during the material damage are investigated.

2 MATERIAL AND METHOD

Table 1. Mixture composition (amount used to obtain 3 beams 4x4x16cm).

Symbol	CM0	CM0.1	CM0.2
CEM I 32.5 [g]	450	450	450
Sand [g]	1350	1350	1350
Water [g]	203	203	203
AEA [g]	0	0,45	0,9

The cement mortar recipe is given in Table 1. The composition of aggregate was taken according to EN:196-1:2005. Two different amounts of AEA were added 0.1% and 0.2% of cement mass. W/C ratio of cement mixture is equal to 0.45. After mixing of all ingredients the beams 4x4x16 cm were casted and they were stored in water 28 days. AEA was added to the cement mortar to modify its internal structure and to improve the resistance against growing crystals.

After 28 days curing the cylinders of 0.9 cm diameter and 1.2-1.4 cm height were cut from the beams. They were dried in the oven (70^{o}C) until the constant mass of the samples were reached. After the drying they were stored in the closed vessel with the relative humidity and temperature equal 5-10% and 30±1^{o}C, appropriately. The samples were saturated with sodium sulfate solution in water, whose concentration equals 0.25 kg/kg. Saturated samples were sealed to prevent the solution outflow from pores. Then the samples were put into the climatic chamber. The temperature in the climatic chamber was changing according to the formula:

$$T = \begin{cases} 30 - 5t & ^{\circ}C,\ t = 0..4h \\ 10 & ^{\circ}C,\ t = 4..8h \\ 10 + 5t & ^{\circ}C,\ t = 8..12h \\ 30 & ^{\circ}C,\ t = 12..16h \end{cases} \tag{3}$$

The samples containing sodium sulfate were exposed to ten temperature cycles. The solubility of sodium sulfate considerably

changes with temperature. The cooling induces hydration of salt molecules and Na_2SO_4 $10H_2O$ (mirabilite) is formed. During the warming the deca-hydrate is again dissolved. The incorporation of 10 molecules of water by one salt molecule increases its molar volume up to 219.8 cm^3/mol [9]. During the sodium sulfate hydration the crystallization pressure is released, which acts as the additional internal load on the solid skeleton. The magnitude of crystallization pressure may be estimated using the equation [10]:

$$\Delta p = \frac{RT}{V_m} \ln\left(\frac{a}{a_\infty}\right) - \overline{\gamma}_{cl} \frac{dA}{dV} \tag{4}$$

where R is universal gas constant, T is absolute temperature, V_m is the molar volume, a_∞ is equilibrium activity of the large reference crystal under the ambient pressure, a is the activity of the dissolved salt, $\overline{\gamma}_{cl}$ is the average surface free energy of the crystal–liquid interface. Coefficient dA/dV depends on the shape and the dimension of pores and equals: $2/r$ for the spherical pores, $1/r$ for the cylindrical pores, $4/x$ for the cubic pores, etc. The first term on the right hand side of eq. (4) describes the influence of solution supersaturation on the crystallization pressure and the second term defines the influence of size and shape of pores in which the crystallization takes place. One can notice that the smaller are pores, the smaller is crystallization pressure, which is released by the growing crystal from the supersaturated salt solution of the same concentration. After the crystallization cycles the samples were taken from the climatic chamber, put into the demineralized water at the temperature equal to 30°C. Crystals dissolution and removal of salt from the pore system lasted 2 weeks, during which the water was being changed every day. Such a procedure was designed to get rid of the remaining crystals from the pore system in order to measure the changes of the pure cement mortar microstructure according to the salt crystallization.

3 RESULTS AND DISCUSION

Five samples of each materials taken before and after crystallization test were investigated using multi-cycle MIP. The results for samples with the higher and the lower porosity were rejected and are not analyzed in the paper.

3.1 Cement mortar without admixture

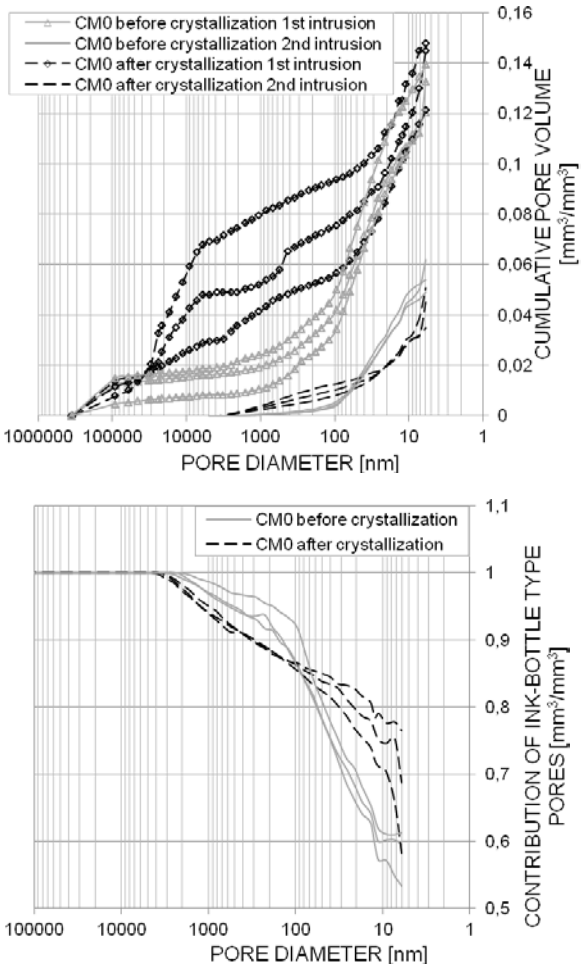

Figure 1. Comparision of a) cumilative pore volume and b) contribution of ink-bottle type pores obtained in MIP for CM0 samples before and after the crystallization test.

The average total porosity before the crystallization test equals 13,1% and after the test to 13,8%. Comparing the pore size distribution – Figure 1a and the contribution of ink-bottle type pores, see Figure 1b, the reader can find the important difference between the samples microstructure before and after the crystallization test. The dissimilarity concerns the pores of diameter from 20 nm up to 30 μm.

In that range the samples after crystallization test contain 2-3.5 times more volume than the samples before the test. These range of diameters of affected pores corresponds to the capillary pores, which play the major role in the transport phenomena [11]. This observation is confirmed by the analysis of the contribution of ink bottle-type pores. For the pores of diameter 0.1-2 μm the contribution of ink-bottle type pores in the sample after crystallization test is lower than in the sample before the test. It can be explained by the fact that the thin channels, which connect the larger pores are broken. The volume of pores, whose diameter is smaller than 50 nm, decreased during the test. The contribution of ink-bottle type pores increases with the progress of salt crystallization. Those phenomena may be explained by the fact that the entrance to the smaller pores was blocked with the damaged parts of the skeleton, building the walls of larger pores or the parts of the undissolved crystals still remaining in the pore system.

3.2 Cement mortar with 0.1% AEA

It can be noticed that the average total porosity of samples before the test equals 14.7% and after the test 14.0%. The decrease of total porosity during the crystallization may be caused by the damage of internal structure of material, which manifests by the closing the entrances to the smaller pores by parts of broken skeleton, making them inaccessible for mercury. The curves measured for the samples after the test are very similar, therefore one can conclude that the results, describing the behavior of the material under the cycling crystallization, are representative. Cumulative pore volume obtained during first and second mercury intrusion for CM0.1 samples before and after crystallization test is presented in Figure 2a. The comparison of the contribution of ink-bottle type pores for those two kind of CM0.1 samples is shown in Figure 2b. The dissimilarity between the measured cumulative pore volume for affected and unaffected samples refers only to the pores of diameter from 0.1 to 10 μm.

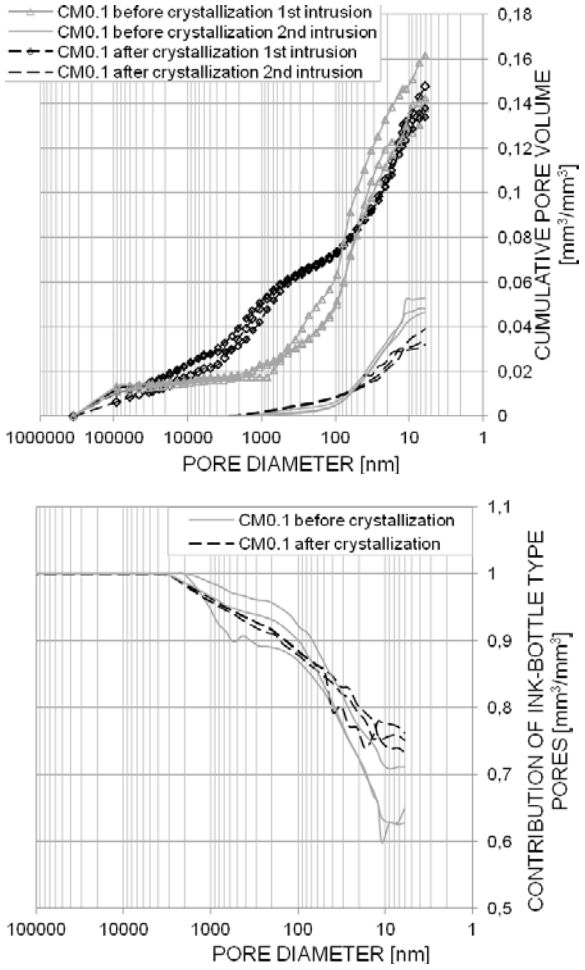

Figure 2. Comparision of a) cumilative pore volume and b) contribution of ink-bottle type pores obtained in MIP for CM0.1 samples before and after the crystallization test.

The difference between the cumulative pore volume obtained for the above mentioned pore range is smaller than measured for CM0 samples and does not exceed 150%. The crystals growing in the pores of CM0.1 samples have almost no influence on the contribution of the ink-bottle type pores. Only channels of diameter between 20-30 μm are broken due to salt crystallization. The average total contribution of ink-bottle type pores in affected samples is slightly higher than for unaffected ones and equals: 66% and 75% appropriately. It may serve as a confirmation of the fact that the entrance to the smaller pores are closing by the damaged parts of the solid skeleton.

3.3 Cement mortar with 0.2% AEA

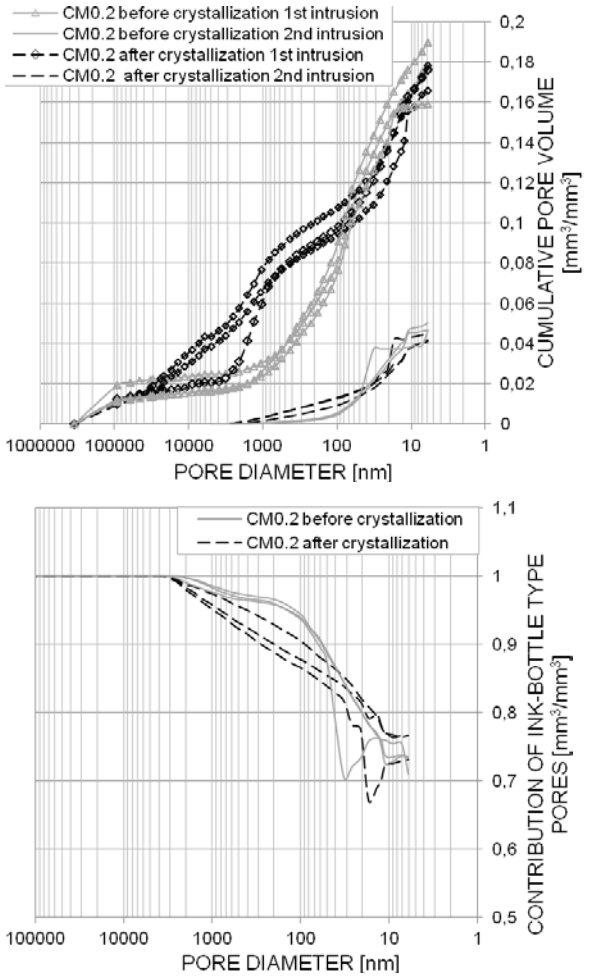

Figure 3. Comparision of a) cumilative pore volume and b) contribution of ink-bottle type pores obtained in MIP for CM0.2 samples before and after the crystallization test.

The average total porosity before the crystallization test equals 17.5% and after the test 17.3%. The distribution of pore volume is very similar for all analyzed affected and unaffected samples. The similarity can be clearly noticed for the first mercury intrusion. The changes in the pore structure are most evident for pores, whose diameter ranges from 0.06-20 μm – Figure 3a. The porosity of the samples after the crystallization test, estimated for pore diameter equal to 1μm, is about 150% higher than before the test. The contribution of ink-bottle type pores is very similar for samples before and after the test. The salt crystallization causes partly destruction of the narrow channels, with diameter of 0.06-0.6 μm, connecting the pores – Figure 3b.

4 CONCLUSIONS

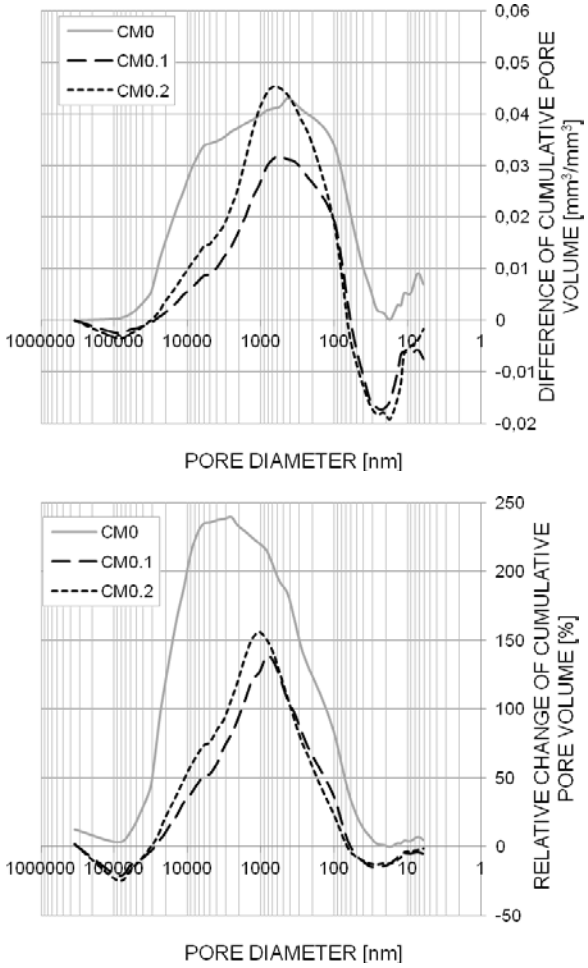

Figure 4. Difference of average cumulative pore volume of CM0, CM0.1, CM0.2 samples before and after the crystallization test.

Internal damage of cement mortar caused by the salt crystallization was investigated in the paper. Change of internal pore structure was measured using the multi-cycle mercury intrusion test, which allows to estimate the contribution of ink-bottle type pores. The pore size is underestimated and one can expect the higher content of larger pores. Consequently the method overestimates the content of smaller pores. Three types of cement mortar were analyzed: without AEA, and containing 0.1% and 0.2% AEA. The significant changes of pore structure are observed for pores (channel connecting pores) of diameter smaller than 30 μm. The higher content of AEA the

higher contribution of ink-bottle type pores is. The multi-cycle MIP analysis gives information about the dimension of the channels between the capillary pores, which play the major role during the mass transport, and therefore the obtained results may be utilized during the estimation of the transport coefficients (permeability, diffusivity, etc.).
During the designed experimental, the damage of cement-based materials microstructure is induced by the salt crystallization. The changes of the average cumulative pore volume of CM0, CM0.1, CM0.2 affected by the salt crystallization referenced to the unaffected ones are presented in Figure 4a. The range and magnitude of internal structure damage is most evident in Figure 4b, where the relative change of pore volume is shown. The most extensive damage of microstructure is observed for cement mortar without admixture.

Acknowledgments

Scientific research was financially supported by the National Science Center, within the grant: UMO-2011/03/B/ST8/05963.

REFERENCES

[1] Monteiro, P.J.M., Kirchheim, A.P., Chae, S., Fischer, P., MacDowell, A.A., Schaible, E., and Wen, H.R., 2009. Characterizing the nano and micro structure of concrete to improve its durability. *Cement and Concrete Composites* **31**:577–584.

[2] Mallidi, S.R., 1996. Application of mercury intrusion porosimetry on clay bricks to assess freeze-thaw durability. *Construction and Building Materials* **10**:461-465,

[3] Kaufmann, J., 2010. Pore space analysis of cement-based materials by combined Nitrogen sorption – Wood's metal impregnation and multi-cycle mercury intrusion. *Cement and Concrete Composites* **32**:514–522.

[4] Zeng, Q., Li, K., Fen-Chong, T. and Dangla, P., 2012. Analysis of pore structure, contact angle and pore entrapment of blended cement pastes from mercury porosimetry data. *Cement and Concrete Composites* **34**:1053–1060.

[5] Washburn, E.W., 1921. Note on a method of determining the distribution of pore size in a porous material. *Proc. Natl. Acad. Sci. USA.* **7**(4):115–116.

[6] Diamond, S., 2000. Mercury porosimetry: An inappropriate method for the measurement of pore size distributions in cement-based materials. *Cement and Concrete Research* **30**:1517-1525.

[7] Kaufmann, J., Loser, R. and Leemann, A., 2009. Analysis of cement-bonded materials by multi-cycle mercury intrusion and nitrogen sorption. *Journal of Colloid and Interface Science* **336**:730–737.

[8] Koniorczyk, M., 2012. Salt transport and crystallization in non-isothermal, partially saturated porous materials considering ions interaction model. *International Journal of Heat and Mass Transfer* **55**:665–679.

[9] Steiger, M. and Asmussen, S., 2008. Crystallization of sodium sulfate phases in porous materials: The phase diagram $Na_2SO4–H_2O$ and the generation of stress, *Geochimica et Cosmochimica Acta* **72**:4291–4306.

[10] Steiger, M., 2005. Crystal growth in porous materials-II: Influence of crystal size on the crystallization pressure. *Journal of Crystal Growth* **282**:470-481.

[11] Kurdowski, W., 2010. *Chemistry of Cement and Concrete* (in Polish), Polski Cement, PWN.